



Received on 11 June 2024; received in revised form, 26 June 2024; accepted, 17 July 2024; published 01 November 2024

SYNTHESIS AND CHARACTERIZATION OF NOVAL SCHIFF BASE COMPLEXES OF MN(II), CO(II), NI(II), CU(II), ZN(II), PD(II), PT(II) METAL IONS FOR MICROBIAL ACTIVITIES AND THEIR NANOPARTICLES

Manisha G. Kapade, Pooja P. Batawale, Uttara M. Dalvi and Manohar V. Lokhande *

Department of Chemistry, Sathaye College (Autonomous), Vile Parle East, Mumbai - 400057, Maharashtra, India.

Keywords:

FTIR, Mass-spectra, UV-Visible, TGA/DTA, SEM, TEM, and EDX

Correspondence to Author:

Prof. (Dr.) Manohar V. Lokhande

Head, Department of Chemistry,
Sathaye College (Autonomous),
Vile Parle East, Mumbai - 400057,
Maharashtra, India.

E-mail: manohar2210@gmail.com

ABSTRACT: New Schiff base metal ion complexes are synthesized and characterized by Mass, TGA, DTA, FTIR, UV-Visible, Conductivity, Magnetic properties, SEM, TEM EDX, and Elemental Analysis. The complexes have the general formula $[ML_2 \cdot H_2O]$, where $L=3-\{(Z)-[(2\text{-aminophenyl})\text{methylidene}] \text{amino}\}-4\text{-chlorobenzoic acid}$, and $M= \text{Mn(II), Co(II), Ni(II), Cu(II), Zn(II), Pt(II), and Pd(II)}$. The Schiff base's imino, amine, and carboxylic groups form a bond, the bands observed in the FTIR of the complexes. UV-Visible spectra of the complexes show that they are colour except for Zn(II) complexes. The parameters like the Nephelauxetic effect, covalence parameter $b^{1/2}$, and co-valence ($\delta\%$) are calculated. The complexes are covalent. The central metal ions have eight coordination numbers, and the ligand behaves as bidentate. According to SEM TEM, EDX, and elemental analysis of the complexes, the size of prepared nanoparticles is 16-84 nm. The mass spectra of the ligand and complexes match the theoretically estimated values of Schiff bases and complexes. According to TGA and DTA complexes decompose when temperature rises, and two coordinated water molecules are present in the coordination sphere. The gram-positive and gram-negative bacteria have been used to screen Ligand and their complexes show an inhibitory effect.

INTRODUCTION: Schiff bases were easily made by condensing real carbonyl groups through primary amines, and they fit into the same appealing class of chemical compounds¹⁻³. By adjusting the aldehydes/ketones and primary amines, it is simple to fine-tune the physicochemical features of Schiff bases and their transition metal complexes⁴⁻⁶.

Because Schiff bases are stable in a variety of settings, one of their key characteristics is their capacity to build the coordination capability of transition metal ions⁷⁻⁸. In metal complexes generated from Schiff bases, the coordination sphere's surrounding environment may be modified by substituting several species that are suited for forming the preferred steric and electrical characteristics⁹.

Due to their adaptability, versatility, and wide range of applications¹⁰⁻¹¹, Schiff bases chemistry is becoming a more significant and comprehensive study area. They can bind a variety of metal ions to create complexes thanks to their multifunctional

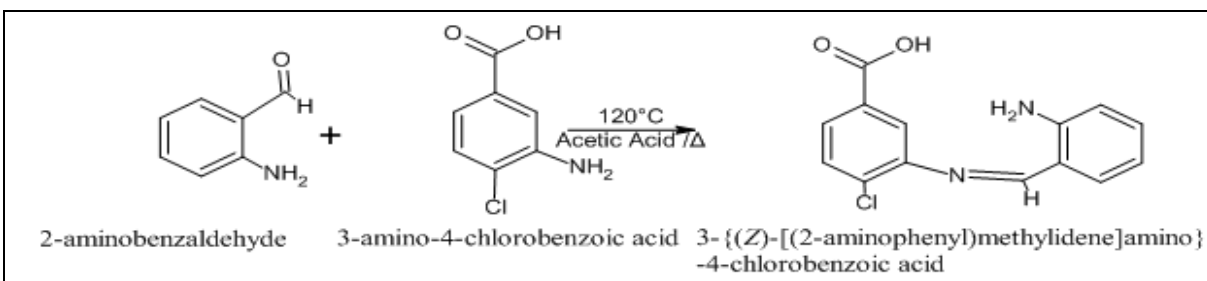
<p>QUICK RESPONSE CODE</p>	<p>DOI: 10.13040/IJPSR.0975-8232.15(11).3297-06</p> <hr/> <p>This article can be accessed online on www.ijpsr.com</p> <hr/> <p>DOI link: https://doi.org/10.13040/IJPSR.0975-8232.15(11).3297-06</p>
-----------------------------------	--

structures and capabilities¹²⁻¹³. Imino or diamino groups of Schiff bases with OH groups in orthogonal positions to amino groups are given more attention¹⁴⁻¹⁵. Their metal complexes exhibit potent antibacterial and antifungal properties¹⁶⁻¹⁷, antioxidant properties¹⁸, anticancer properties¹⁹, anti-inflammatory properties²⁰, and catalytic properties²¹. In this research paper, we synthesized Schiff bases and their transitional metal ion complexes.

MATERIALS AND METHODS: Without additional and further purification, AR, LR-grade chemicals, and reagents were used. Mark Chemicals supplied 3-amino-4-chlorobenzoic acid, Lobo Chemicals provided 2-amino benzaldehyde,

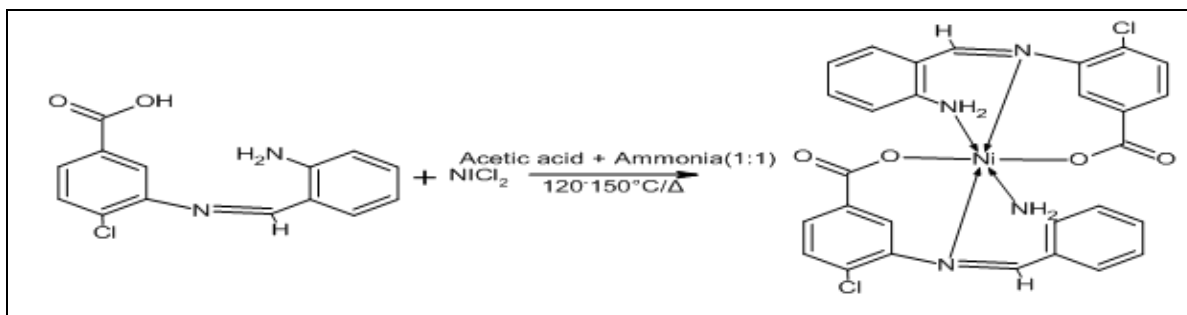
and SD Fine Chemicals supplied metal chlorides and nitrates

Synthesis of Schiff Base: In a 25 cm³ flask, 1.71g of 3-amino-4-chlorobenzoic acid and 1.21g of 2-amino benzaldehyde were individually dissolved in 100% alcohol. The two solutions were then combined in a 250 cm³ round-bottom flask. Following the mixing of these solutions, a water condenser was used to reflux them for three hours at 120°C. During this time, two to three drops of 1M acetic acid were added. The final solution was allowed to cool to ambient temperature after three hours. After obtaining the solid precipitate, it was filtered with Whatman filter paper-41 and dried in a hot air oven at 60 °C. The product has a 93% yield.



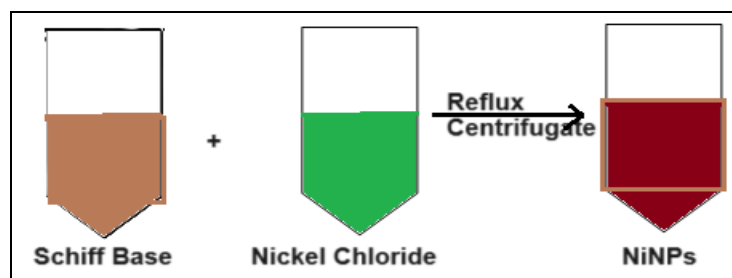
Synthesis of Metal Ion Complexes: Double distilled alcohol was used to create the [3-[(Z)-(2-aminophenyl) methylidene]- amino}-4-chloro benzoic acid (0.02M) solution, and double distilled water was used to prepare the metal chloride solutions [M= Mn (II), Co(II), Ni(II), Cu(II), Zn (II), Pt(II), and Pd(II)]. Using a water condenser, the equi-molar concentration solutions of Schiff base (0.02M) and metal chloride (0.02M) were refluxed for 2.00–2.30 hours on a hot plate while

being continuously stirred by a magnet. Two to three drops of alcoholic ammonia (1:1) were applied dropwise during refluxing, and different metal ions aside from zinc (II) ions produced varied coloured precipitates. This precipitate was allowed to cool, filtered, and then cleaned with 50% pure alcohol and distilled water. These complexes were dried for two hours at 70 °C in a dry hot air oven. The resulting complex gives up to 65-78 % of the yield.



Synthesis of Nanoparticles: The synthesis of nanoparticles was carried out by mixing a metal ions solution with Schiff base at an equimolar concentration of 0.02M. The mixture was then refluxed for three hours, transferred to a test tube, and centrifuged in a machine at room temperature

for over three hours at 5000 RPM. Coloured crystals' excellent power was attained. Following their separation and drying, these crystals were kept at room temperature in a covered container. The purpose of these nanoparticles was characterization.



Characterization: Measurements of magnetic susceptibility were performed using $\text{HgCO}(\text{CNS})_4$ as a calibrant. Using KBr pellets, FTIR was recorded on a Perkin Elmer FTIR -8400 Spectrometer ($4000\text{-}400\text{cm}^{-1}$). A Cintra-5 GBC UV-visible spectrophotometer was used to record UV-visible spectra. On a Mettler Toledo Star System, TGA (thermogravimetric analysis) and DTA (differential thermal analysis) measurements were made between 50°C and 1000°C when atmospheric nitrogen was present. Using the Maxis Impact (Bruker) mass spectrometer, ligand and complexes mass spectra were taken. An Elico conductivity bridge was used to test conductivity. SEM and TEM data were obtained at the nanoparticles because it finds dispersed electrons on the particle surface by using Quanta 200 ESEM is the instrument by Icon Laboratory Mumbai, An elemental analysis was carried out in the laboratory.

RESULT AND DISCUSSIONS: The table below lists the Schiff base complexes' analytical and physical parameters. All complexes are coloured and thermally stable at room temperature, with the exception of Zn(II). While complexes are soluble in DMSO and DMF, the Schiff base is soluble in ethanol, methanol, butanol, acetone, and benzene. The complexes broke down at high range temperatures between 237 and 254°C , whereas the Schiff bases melted between 175 and 178°C . The MP and DP were obtained in an uncorrected open capillary setting. The complexes were shown to be non-electrolytic based on their molar conductance measurements in DMSO at 10^{-3} M concentration²²⁻²³. Pd(II) and Pt(II) were measured using AAS techniques, and the metal concentrations were determined using 0.01M EDTA with various indicators²⁴.

TABLE 1: PHYSICAL AND ANALYTICAL PARAMETERS (*EXPERIMENTAL)

Schiff base/ Complexes	% Yield	MP/ DP $^\circ\text{C}$	C%	N%	M%	$\Omega^{-1}\text{ol}^{-1}\text{cm}^2$	BM, μ_{eff}
($\text{C}_{14}\text{H}_{11}\text{ClN}_2\text{O}_2$)	93	175-178	61.21 60.85*	10.20 10.03*	- -	-	-
$[\text{Mn}(\text{C}_{28}\text{H}_{20}\text{Cl}_2\text{N}_4\text{O}_4).2\text{H}_2\text{O}]$	72	241-244	52.68 52.40*	07.78 07.59*	08.61 08.38*	4.38	5.28
$[\text{Co}(\text{C}_{28}\text{H}_{20}\text{Cl}_2\text{N}_4\text{O}_4).2\text{H}_2\text{O}]$	75	245-248	52.37 52.17*	07.72 07.58*	09.17 09.01*	4.44	4.22
$[\text{Ni}(\text{C}_{28}\text{H}_{20}\text{Cl}_2\text{N}_4\text{O}_4).2\text{H}_2\text{O}]$	68	250-253	52.17 52.02*	08.73 08.59*	09.14 08.98*	4.98	3.30
$[\text{Cu}(\text{C}_{28}\text{H}_{20}\text{Cl}_2\text{N}_4\text{O}_4).2\text{H}_2\text{O}]$	65	247-250	51.98 51.82*	08.66 08.51*	09.82 09.68*	5.01	1.80
$[\text{Zn}(\text{C}_{28}\text{H}_{20}\text{Cl}_2\text{N}_4\text{O}_4).2\text{H}_2\text{O}]$	78	240-243	51.83 51.70*	08.64 08.48*	10.08 09.92*	4.98	Dimag
$[\text{Pt}(\text{C}_{28}\text{H}_{20}\text{Cl}_2\text{N}_4\text{O}_4).2\text{H}_2\text{O}]$	69	248-251 243-246	43.20 43.05*	07.20 07.02*	25.06 24.90*	4.92	-
$[\text{Pd}(\text{C}_{28}\text{H}_{20}\text{Cl}_2\text{N}_4\text{O}_4).2\text{H}_2\text{O}]$	71		48.75 48.59*	08.12 07.98	15.43 15.27*	4.97	-

Infrared Spectra: IR spectra offer important insights into the characteristics of a functional group that is joined to a metal atom. To investigate metal complexes using the Schiff coupling mode base. Table 2 data of pertinent infrared bands that offer strong structural support for the ligand and

complexes formation. The ligand and its substituted moieties were compared with the complexes' infrared spectra. All metal complexes have large bands assigned to them in the infrared spectrum 3489 cm^{-1} and 3414 cm^{-1} , which suggests the existence of two coordinated water molecules.

The $>C=N$ - vibration is the cause of the band at 1642 cm^{-1} in the free Schiff base. This group's shift in metal complexes to a lower frequency (1606 – 1529 cm^{-1}). When contrasted to the free ligand in metal complexes, indicates that the nitrogen atom azomethine group coordinates the metal ion²⁵⁻²⁶.

The Schiff base's amino group peak, which is located at 3391 cm^{-1} , will be moved to lower frequencies in complexes that fall between 3136 cm^{-1} . The atom would reduce the azomethine bond's electron density, which would reduce HC=N -absorption.

In any metal complex when the oxygen atom of the carboxylic group is involved in the bond with metal ions (deprotonation of the carboxylic group), the band at 3385 cm^{-1} is attributed to the carboxylic ion²⁷. The complexes' spectra showed new bands

absent from the ligand's spectrum in the range 574 – 550 cm^{-1} bands corresponding to $\nu_{\text{M-N}}$ and 475 – 492 cm^{-1} to $\nu_{\text{M-O}}$ vibrations, respectively²⁸⁻²⁹. These bands supported the involvement of carboxylic groups of oxygen, nitrogen of azomethine, and amino group complexation with metal ions³⁰.

In complexes in the 1307 cm^{-1} , the frequency of the ligand's carboxylic stretching is seen at 1318 cm^{-1} and is moved to a lower frequency area, indicating bonding via carboxylic oxygen.

Thus, $>C=N$ -, amino and $-\text{COO}^-$ are the coordination sites of the metal ion, as shown by the IR spectrum data. The central metal ions have eight coordination numbers and the ligand behaves as bidentate³¹.

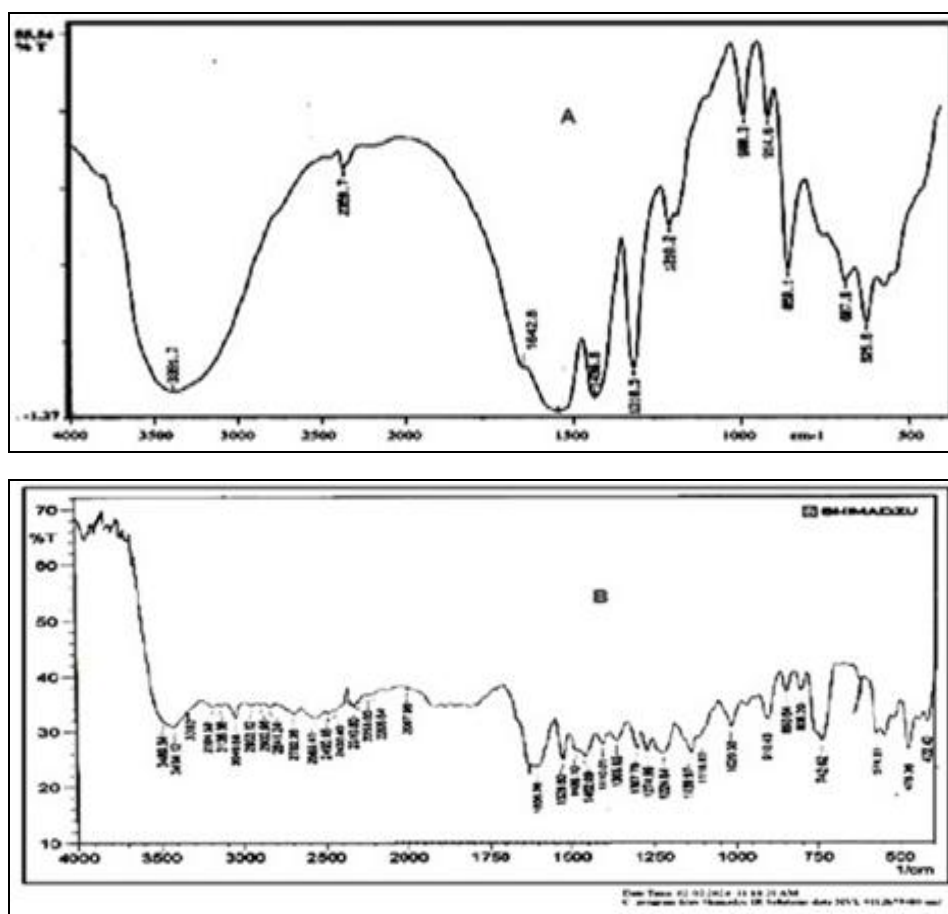


FIG. 1: IR OF (A) SCHIFF BASE AND (B) NI(II) COMPLEX

SEM, TEM and EDX: The SEM, TEM, and EDX micrographs of complexes are shown below figures. The SEM and TEM images of these complex molecules are arranged in granular shape

with spherical shape structure³². The particle size of the prepared complexes is between 16-84 nm. EDX analysis shows that the complex has corrected elements that are present in prepared complexes.

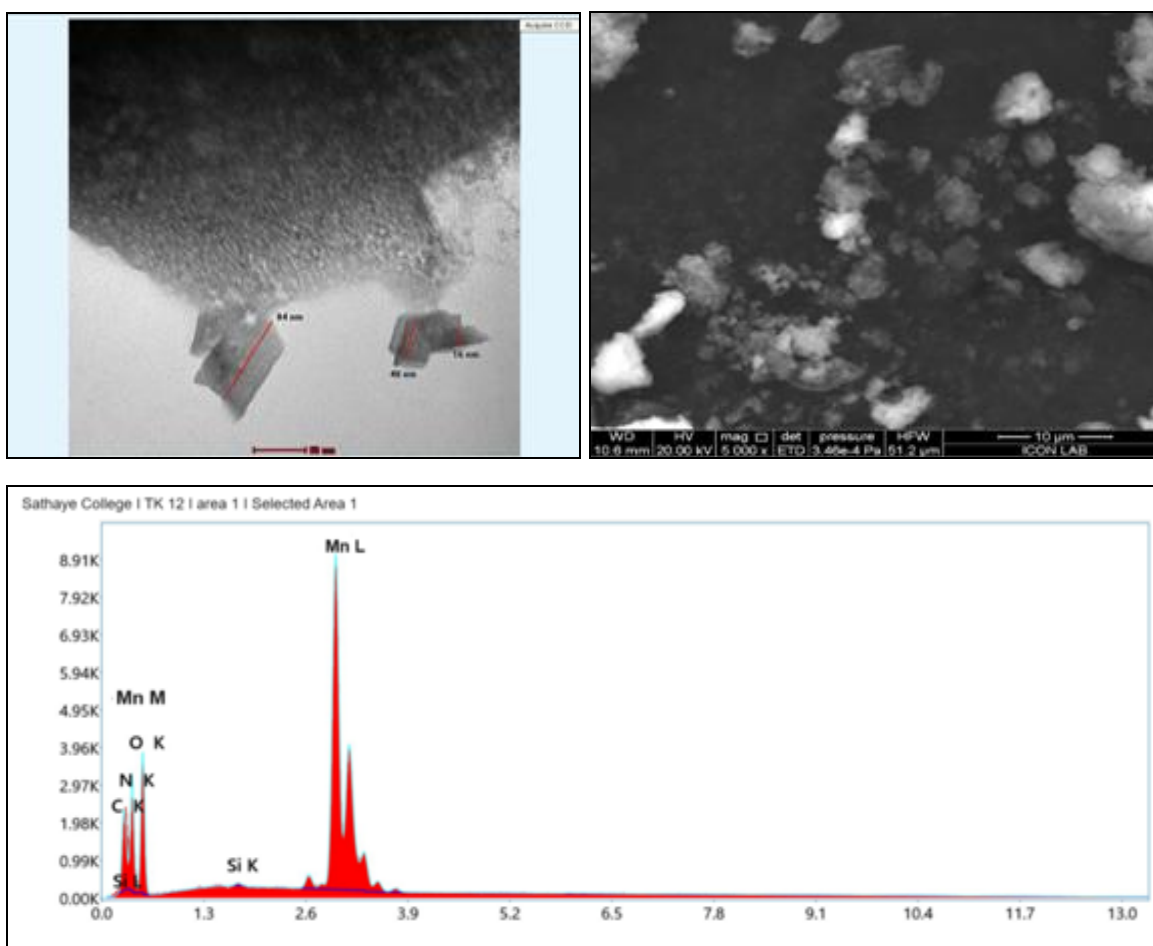


FIG. 2: SEM, TEM AND EDX OF MN(II) COMPLEX

Electronic Spectra: The assessment of outcomes provided by alternative structural inquiry techniques frequently benefits greatly from the use of electronic absorption spectra. Based on the locations and quantity of d-d transition peaks, the stereochemistry of the metal ions in the complexes was determined using electronic spectrum measurements³³.

Using acetone as a solvent, the electronic absorption spectra of the Schiff base and its Mn(II), Ni(II) and Cu(II) complexes were recorded at ambient temperature. In the electronic spectra of the Cu(II) complex, a single wide band is seen at $16,666\text{ cm}^{-1}$ (600 nm) and $25,974\text{ cm}^{-1}$ (385 nm), corresponding to the ${}^4\text{T}_{1g} \rightarrow {}^4\text{A}_{2g}(\text{P})$, and ${}^4\text{T}_{1g} \rightarrow {}^4\text{T}_{2g}$ transitions, respectively. These transitions are

consistent with octahedral geometry. The Mn(II) complex's electronic spectra revealed two spin-allowed transitions at $12,315\text{ cm}^{-1}$ (812 nm), $17,856\text{ cm}^{-1}$ (560 nm), and $21,734\text{ cm}^{-1}$ (460 nm), respectively. These transitions are attributed to ${}^4\text{T}_{1g} \rightarrow {}^4\text{T}_{2g}(\text{F})$, ${}^4\text{T}_{1g} \rightarrow {}^4\text{A}_{2g}(\text{F})$, and ${}^4\text{T}_{1g} \rightarrow {}^4\text{T}_g(\text{P})$, and they are consistent with the octahedral arrangements for the Co(II) ion.

An octahedral geometry for the Ni(II) complex is supported by the emergence of a band at $24,509\text{ cm}^{-1}$ (408 nm), $19,230\text{ cm}^{-1}$ (520 nm), and $13,123\text{ cm}^{-1}$ (762 nm) due to its assignments ${}^3\text{A}_{2g} \rightarrow {}^3\text{T}_{1g}(\text{P})$, ${}^3\text{A}_{2g} \rightarrow {}^3\text{T}_{1g}$ and ${}^3\text{A}_{2g} \rightarrow {}^3\text{T}_{2g}$ transitions³⁴⁻³⁵. The nephelauxetic effect, covalence parameter $b^{1/2}$, and co-valence ($\delta\%$) parameters were calculated^{36 & 11} and listed in the below table.

TABLE 2: ELECTRONIC SPECTRA

Complexes	Bands (nm)	β	$1-\beta$	η	$b^{1/2}$	$\delta\%$
[Co(C ₂₈ H ₂₀ Cl ₂ N ₄ O ₄). 2H ₂ O]	382,590	0.9775	0.0225	0.0116	0.1060	1.1662
[Ni(C ₂₈ H ₂₀ Cl ₂ N ₄ O ₄). 2H ₂ O]	450,530,645	0.9798	0.0202	0.0104	0.1004	1.0410
[Cu(C ₂₈ H ₂₀ Cl ₂ N ₄ O ₄). 2H ₂ O]	432,542	0.9802	0.0198	0.0102	0.0994	1.0201

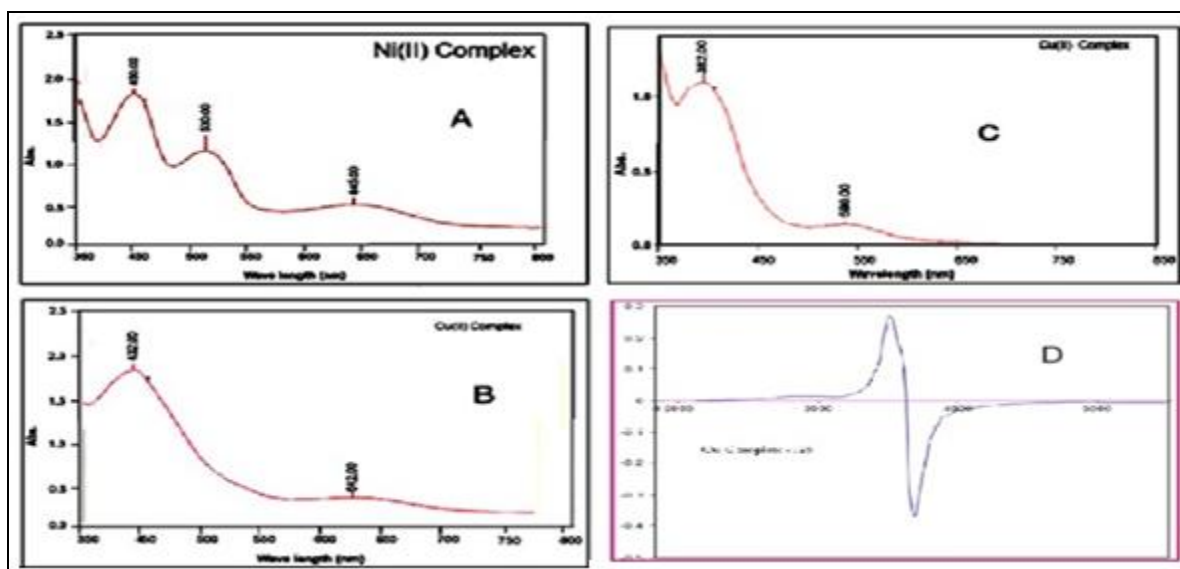


FIG. 3: UV-VISIBLE OF A) NI(II), B) CU(II), C) CO(II) COMPLEXES AND D) ESR SPECTRA OF CU(II) COMPLEX

ESR Spectra: The distribution of unpaired electrons and consequently, the kind of bonding between the metal ion and its ligands are revealed by ESR spectrum analysis of paramagnetic transition metal (II) complexes. Many publications have been published on the use of ESR to analyze square-planar or deformed octahedral complexes of $[\text{Cu}(\text{C}_{28}\text{H}_{20}\text{Cl}_2\text{N}_4\text{O}_4) \cdot 2\text{H}_2\text{O}]$ and how the covalency of the metal-ligand bonding is interpreted based on the ESR parameters³⁷.

As seen in figure the Cu(II) complex displayed nicely resolved anisotropic signals in both the parallel and perpendicular areas. The table displays the observed data, which indicates that $g_{\parallel} = 2.37$ and $g_{\perp} = 2.0928$. The Cu(II) complex appears to have significant distortion from octahedral symmetry, as shown by the g_{\parallel} values being larger than g_{\perp} ³⁸.

The function g_{\parallel} is somewhat sensitive to covalency. In M-L bonding, an anionic environment is characterized by $g_{\parallel} > 2.4$ and a covalent environment by $g_{\parallel} < 2.4$. The Cu(II) complex's measured g_{\parallel} values are smaller than 2.4, which is consistent with the M-L bond's covalent nature. On the other hand, the Cu(II) complex displayed $g_{\parallel} > 2.4$, a feature indicative of an anion environment. The complexes exhibit a trend of $g_{\parallel} > g_{\perp} > 2.0020$, indicating that the unpaired electron is located in the dx^2-y^2 orbital of the Cu(II) ion. For the complexes, a tetragonal shape is therefore suggested³⁹.

The exchange interaction between the metal centers in a polycrystalline solid is measured by the axial symmetry parameter $G = (g_{\parallel} - 2)/(g_{\perp} - 2)$, which has been determined. If $G > 4$, there is little exchange interaction, and if $G < 4$, there is significant exchange interaction in the complexes.

Mass Spectra: To examine the stoichiometry composition of the $(\text{C}_{14}\text{H}_{11}\text{ClN}_2\text{O}_2)$ Schiff base and its metal complexes, room-temperature ESI mass spectra are employed. The [M] peak's estimated m/z of 274.70 matches to the Ligand [L] molecular ion peak at m/z 274.7. While the mass spectra of the two compounds, $[\text{Ni}(\text{C}_{28}\text{H}_{20}\text{Cl}_2\text{N}_4\text{O}_4) \cdot 2\text{H}_2\text{O}]$ shows theoretical m/z is 642.08 and $[\text{Mn}(\text{C}_{28}\text{H}_{20}\text{Cl}_2\text{N}_4\text{O}_4) \cdot 2\text{H}_2\text{O}]$ is 612.28 m/z respectively, which corresponds to the molecular weight of the respective compounds. These peaks attest to the complexes' structural integrity and validate the metal chelates' $[\text{ML}_2]$ type stoichiometry.

The fragmentation of the metal complex molecule resulting from the rupture of various bonds inside the molecule by successive degradation is responsible for the various molecular ion peaks that appear in the mass spectra of complexes. This formation of various radicals leads to the formation of many more significant peaks⁴⁰. Molecular ion peaks in complex spectra are consistent with the structure inferred from elemental analysis, spectroscopic, and magnetic investigations.

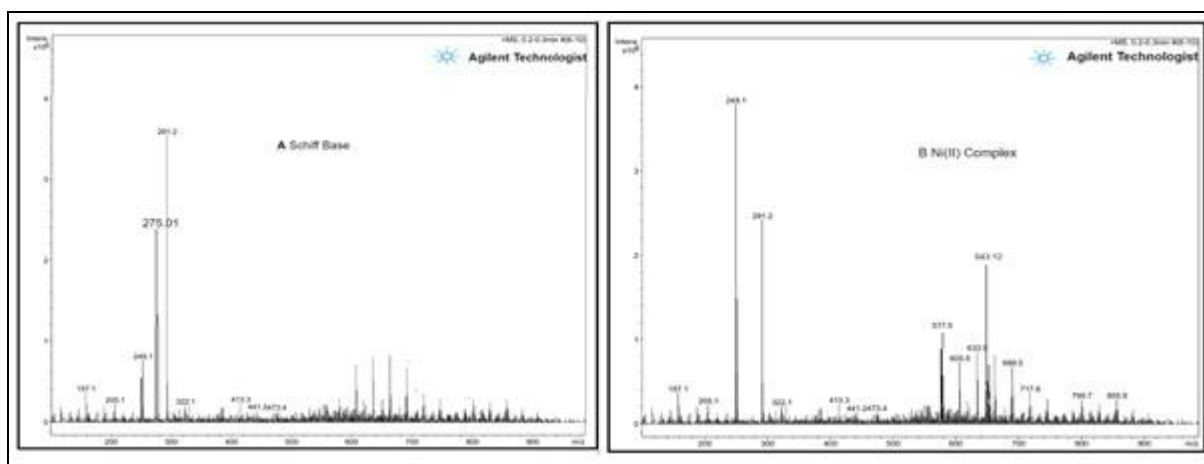


FIG. 4: MASS SPECTRA OF A) SCHIFF BASE AND B) NI(II) COMPLEX

TGA/DTA: The findings of the differential thermal analysis and thermogravimetric analysis of $[\text{Pt}(\text{C}_{28}\text{H}_{20}\text{Cl}_2\text{N}_4\text{O}_4) \cdot 2\text{H}_2\text{O}]$ are presented as below. Because of the exothermic and endothermic processes, complexes lose weight. These compounds break down in several stages and are thermally stable at room temperature. The Pt(II) Complex breaks down into four stages. In the first stage, one water molecule and a portion of the chelate are lost at temperatures between 30-135 °C. The organic moiety and another water molecule are lost at temperatures

between 135-295 degrees Celsius. The mass loss corresponds to the formation of intermediate species through the decomposition of some part of the complex's organic moiety in between 300-425 °C and finally the complex decomposition is caused and formed by the metal oxides at higher temperatures, specifically in the 430-775 °C temperature range. This process continues until a constant weight is reached, at which point a mixture of manganese oxide residue is produced. The above complex's decomposition is illustrated in as below;

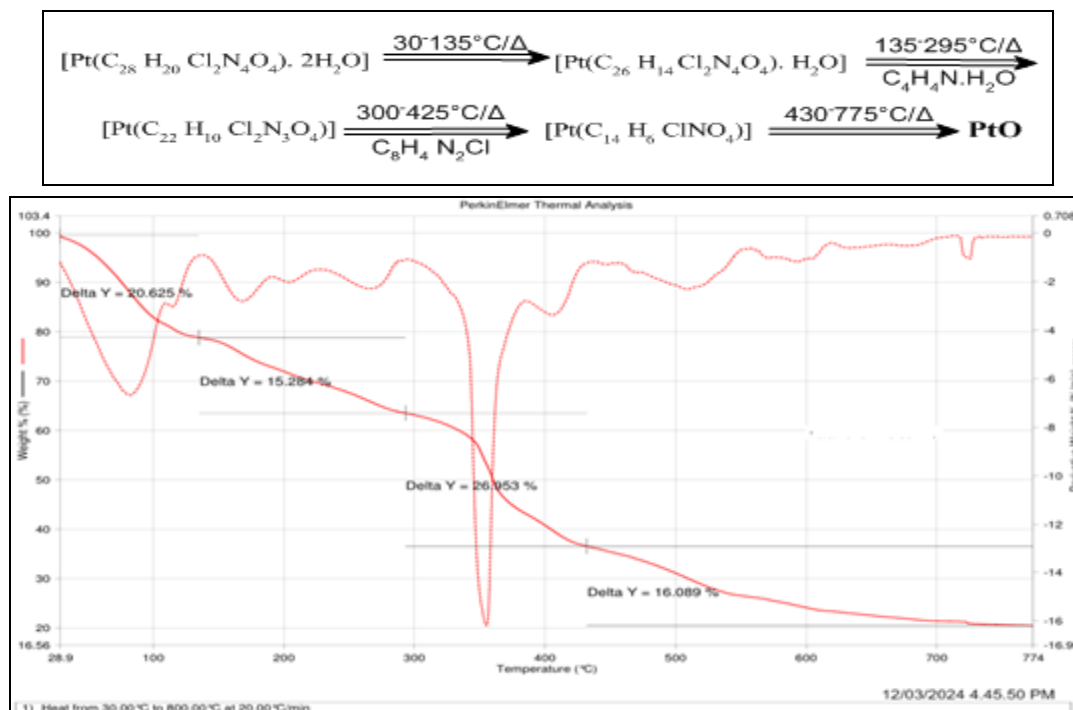


FIG. 5: TGA DTA OF PT (II) COMPLEX

Microbial Activity: The Schiff base Ligand(L-1) shows less activity against all the micro-organisms while its Cu(II), Pd(II) and Pt(II) complexes show

higher activities compared to Mn(II) and Ni(II) complexes. The Mn(II) complex shows moderate activities against all bacteria.

TABLE 3: MICROBIAL ACTIVITY

Ligand/ Complexes	Gram-Positive Bacteria		Gram-Negative Bacteria	
	<i>S. aureus</i>	<i>B. subtilis</i>	<i>E. coli</i>	<i>S. typhi</i>
(C ₁₄ H ₁₁ ClN ₂ O ₂)	14	17	15	17
Mn(II) Complex	17	19	18	20
Ni(II) Complex	18	20	19	21
Cu(II) Complex	22	24	23	26
Pd(II) Complex	21	23	22	24
Pt(II) Complex	23	27	24	26

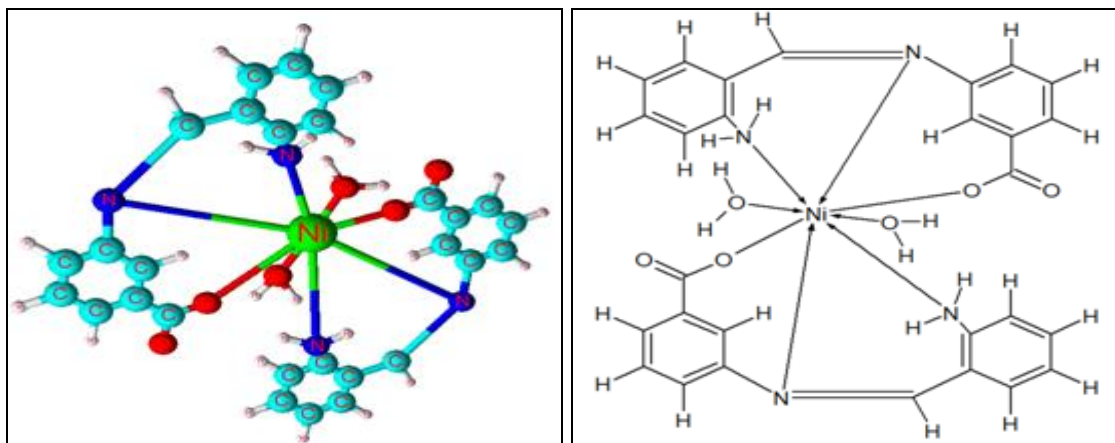


FIG. 6: COMPLEX STRUCTURE

CONCLUSION: Using a condensation reaction, 3-((Z)-[(2-aminophenyl) methylidene] amino)-4-chlorobenzoic acid was converted into Schiff base with their metal ion complexes created. The link between the nitrogen of the imino, amino groups and the oxygen of the carboxylic group was shown bonding with metal ions in the IR spectra of the complexes. The complexes are covalent. The central metal ions have eight coordination numbers and the ligand behaves as bidentate. The study also shows that the coordination sphere contains two coordinated water molecules. Cu(II), Co(II), and Ni(II) complexes of the Schiff base and its electronic absorption spectra were recorded and showed covalent bonding. The parameters like the Nephelauxetic effect, covalence parameter $b^{1/2}$, and co-valence ($\delta\%$) are calculated. Cu(II) & Ni(II) complexes had an octahedral geometry with weak covalent bonding. The different ESR spectrum parameters are computed. The complexes' mass spectra match the ligand and complexes' theoretical masses.

ACKNOWLEDGMENTS: The authors would like to thank the Management of PTVA, HOD, Chemistry, and the Principal for providing the necessary research facilities. SEM, TEM, and EDX were recorded at the ICON laboratory, Mumbai TGA/DTA facilities from CMET Pune.

CONFLICT OF INTEREST: No conflicts of interest regarding this investigation.

REFERENCES:

1. Verma R, Lamba NP, Dandia A, Srivastava A, Modi K, Chauhan MS and Prasad J: Synthesis of N Benzylideneaniline by Schiff base reaction using Kinnow peel powder as Green catalyst and comparative study of derivatives through ANOVA techniques. Scientific Reports 2022; 12: 9636. <https://doi.org/10.1038/s41598-022-13360-5>.
2. Maleki A, Hajizadeh Z and Salehi P: Mesoporous halloysite nanotubes modified by CuFe₂O₄ spinel ferrite nanoparticles and study of its application as a novel and efficient heterogeneous catalyst in the synthesis of pyrazole pyridine derivatives. Scientific Reports 2019; 9(1): 1–8. <https://doi.org/10.1038/s41598-019-42126-9>
3. Hajizadeh Z, Radinekiyan F, Eivazzadeh R and Maleki A: Development of novel and green NiFe₂O₄ geopolymer nanocatalyst based on bentonite for the synthesis of imidazole heterocycles by ultrasonic irradiations. Scientific Reports 2020; 10(1): 1–11. <https://doi.org/10.1038/s41598-020-68426-z>.
4. Dasari RR, Haranath C and Ahad HB: Complex Drug Delivery Systems. International Journal of Pharmaceutical Science and Research 2022; 13(4): 1533-1539. [https://doi.org/10.13040/IJPSR.0975-8232.13\(4\).1533-39](https://doi.org/10.13040/IJPSR.0975-8232.13(4).1533-39)
5. Boulechfar C, Ferkous H, Delimi A, Djedouani A, Kahlouche A, Boublia A, Darwish AS, Lemaoui T, Verma R and Benguerba Y: Schiff bases and their metal Complexes: A review on the history, synthesis, and applications. Inorganic Chem Communication 2023; 150: 110451. <https://doi.org/10.1016/j.inoche.2023.110451>.
6. Kaur M, Kumar S, Younis SA, Yusuf M, Lee J, Weon S, Kim KH and Malik AK: Post-synthesis modification of metal-organic frameworks using Schiff base complexes for

- various catalytic applications. *Chemical Engineering Journal* 2021; 423: 130230. <https://doi.org/10.1016/j.ccej.2021.130230>.
7. Zhao S, Song X, Song S and Zhang HJ: Highly efficient heterogeneous catalytic materials derived from metal-organic framework supports/precursors. *Coordination Chemistry Review* 2017; 337: 80-96. <https://doi.org/10.1016/j.ccr.2017.02.010>.
 8. Kang YS, Lu Y, Chen K, Zhao Y, Wang and Sun WY: Metal-organic frameworks with catalytic centers: From synthesis to catalytic application. *Coordination Chemistry Review* 2019; 378: 262-280. <https://doi.org/10.1016/j.ccr.2018.02.009>.
 9. Adlinge NP, Jadhav SB and Rathod SD: Synthesis and antimicrobial study of metal complexes of Sm (III), Eu (III) and asymmetrical ligand derived from dehydroacetic acid. *International Journal of Pharmaceutical Science and Research* 2022; 13(7): 2753-2758. [https://doi.org/10.13040/IJPSR.0975-8232.13\(7\).2753-58](https://doi.org/10.13040/IJPSR.0975-8232.13(7).2753-58)
 10. Venkatesh G, Vennila P, Kaya S, Ahmed SB, Sumathi P, Siva V, Rajendran P and Kamal C: Synthesis and Spectroscopic Characterization of Schiff Base Metal Complexes, Biological Activity, and Molecular Docking Studies. *ACS Omega* 2024; 9(7): 8123-8138. <https://doi.org/10.1021/acsomega.3c08526>.
 11. Choudhary MR and Lokhande MV: Some transitional metal ions complexes with 3-[(e)-(4-fluorophenyl)methylidene] amino} benzoic acid and its microbial activity. *International Journal of Pharmaceutical Science and Research* 2014; 5(5): 1757-1766. [https://doi.org/10.13040/IJPSR.0975-8232.5\(5\).1757-66](https://doi.org/10.13040/IJPSR.0975-8232.5(5).1757-66).
 12. Lokhande MV and Gulam FM: Spectral Studies of Some Transition Metal Ion complexes with 4[(E)-(Ferrocene-1-Methylidene) Amino] Pyridin-2-ol. *Journal of Applied Chemistry* 2014; 6(6): 36-42. <https://doi.org/10.9790/5736-0663642>.
 13. Chen L, Wang L, Wugai A, Wang B and Tian L: Synthesis, structural characterization, and antibacterial activity of diorganotin complexes of Schiff base derived from 4-(diethylamino)salicylaldehyde and L-tyrosine. *Inorganic Nano-Metal Chemistry* 2020; 50(9): <https://doi.org/10.1080/24701556.2020.1727515>.
 14. Naureen B, Miana GA, Shahid K, Tanveer S and Sarwar A: Iron (III) and zinc (II) monodentate Schiff base metal complexes: Synthesis, characterization and biological activities. *Journal of Molecular Structure* 2021; 1231: 129946. <https://doi.org/10.1016/j.molstruc.2021.29946>
 15. Allothman AA, Al-Farraj ES, Al-Onazi WA, Almarhoon ZM and Al-Mohaimeed AM: Spectral characterization, electrochemical, antimicrobial and cytotoxic studies on new metal(II) complexes containing N2O4 donor hexadentate Schiff base ligand. *Arabian Journal of Chemistry* 2020; 13(2): 3889-3902. <https://doi.org/10.1016/j.arabjc.2019.02.003>
 16. Nagar S, Raizada S and Tripathy N: A review on various green methods for synthesis of Schiff base ligands and their metal complexes. *Results Chemistry* 2023; 6: 101153. <https://doi.org/10.1016/j.rechem.2023.101153>.
 17. Jarrahpour A, Khalili D, Salmi C, Clercq ED and Brunel JM: Synthesis, antibacterial, antifungal and antiviral activity evaluation of some new bis-Schiff bases of isatin and their derivatives. *Molecules* 2007; 12(8): 1720-1730. <https://doi.org/10.3390/12081720>.
 18. Kizikaya H, Dag B, Aral T, Genc N and Erenle P: Synthesis, characterization, and antioxidant activity of heterocyclic Schiff bases. *Journal of the Chinese Chemical Society* 2020; 67(9): 1696-1701. <https://doi.org/10.1002/jccs.202000161>.
 19. Chang Q, Xie Y, Lu X, Zong Z, Zhang E, Cao S and Liang L: In vitro and in vivo antiproliferative activity on lung cancer of two acyl hydrazone based zinc(II) complexes. *Bioorganic Chemistry* 2024; 147: 107422. <https://doi.org/10.1016/j.bioorg.2024.07422>
 20. Shukla S, Mishra AP: Metal complexes used as anti-inflammatory agents: Synthesis, characterization and anti-inflammatory action of VO(II)-complexes. *Arabian Journal Of Chemistry* 2019; 12(7): 1715-1721. <https://doi.org/10.1016/j.arabjc.2014.08.020>.
 21. Manna CK, Naskar R, Bera B, Das A and Mondal TM: A new palladium(II) phosphino complex with ONS donor Schiff base ligand: Synthesis, characterization and catalytic activity towards Suzuki-Miyaura cross-coupling reaction. *Journal of Molecular Structure* 2021; 1237: 130322. <https://doi.org/10.1016/j.molstruc.2021.130322>.
 22. Choure R and Samim SKA: Electrochemical and pharmacological analysis of cu-atropine complex. *International Journal of Pharmaceutical Science and Research* 2024; 15(3): 808-812. [https://doi.org/10.13040/IJPSR.0975-8232.15\(3\).808-12](https://doi.org/10.13040/IJPSR.0975-8232.15(3).808-12).
 23. Ibrahim RB and Saad ST: Cobalt (II) and Nickel (II) complexes with Schiff base derived from 9,10-phenanthrene quinone and 2-mercaptoaniline, synthesis and characterization. *Journal of Medicinal Pharmaceutical Chemistry and Research* 2023; 5: 739-747. <https://doi.org/10.22034/ecc.2023.390880.612>
 24. Sinhaa B, Bhattachary M, Sahab S and Saha S: Spectroscopic Studies and Antimicrobial Evaluation of New Mixed Ligand Mn(II), Ni(II), Cu(II) Complexes Synthesized from an Ionic Liquid-Supported Schiff Base and 1-Methyl Imidazole. *Polycyclic Aromatic Compounds* 2022; 42: 5962-5974. <https://doi.org/10.1080/10406638.2021.1963790>
 25. Lokhande MV: Synthesis and Characterization of Lanthanide (III) Complexes with 2, 4-pyrimidine diamine-5 [(3, 4, 5-trimethoxy phenyl) methyl]. *Asian Journal of Chemistry* 2006; 18(4): 2662-2670.
 26. Gulam FM and Lokhande MV: Electronic Spectra, Thermal Analysis, X-Ray Powder Diffraction and SEM Studies of Organometallic Compound. *International Journal of Scientific Research* 2013; 4(12): 457-460. <https://doi.org/10.36106/IJSR>.
 27. Putaya AN, Ndahi NP, Bello HS, Mala G, Osunlaja AA and Garba H: Synthesis, characterization and antimicrobial analysis of Schiff bases of o-phenylenediamine and 2-aminopyridine-3-carboxylic acid with ofloxacin and their metal (II) complexes. *International Journal of Biological and Chemical Sciences* 2020; 14(1): 263-278. <https://doi.org/10.4314/ijbcs.v14i1.22>.
 28. Al-Fakeh MS, Alsikhan MA and Alnawmasi JS: Physico-Chemical Study of Mn(II), Co(II), Cu(II), Cr(III), and Pd(II) Complexes with Schiff-Base and Aminopyrimidyl Derivatives and Anti-Cancer, Antioxidant, Antimicrobial Applications. *Molecules* 2023; 28: 2555-2574. <https://doi.org/10.3390/molecules28062555>.
 29. Jaziri E, Louis H, Gharbi C, Unimuke TO, Agwamba EC, Mathias GE, Fugita W, Nasr CB and Khedhiri L: Synthesis, X-ray crystallography, molecular electronic property investigation, and leukopoiesis activity of novel 4,6-dimethyl-1,6-dihydropyridin-2-amino nitrate hybrid material. *Journal of Molecular Structure* 2020; 1268:133733.

30. Rajesh R, Navya V and Kumar SK: Importance of drug excipient compatibility studies by using or utilizing or employing various analytical techniques – An overview. *International Journal of Pharmaceutical Science and Research* 2022; 13(9): 3473-3485. [https://doi.org/10.13040/IJPSR.0975-8232.13\(9\).3473-85](https://doi.org/10.13040/IJPSR.0975-8232.13(9).3473-85).
31. Zhong X, Zhongkui L, Shi R, Li Y, Yanhong Z and Li H: Schiff Base-Modified Nanomaterials for Ion Detection: A Review. *ACS Applied Nanomaterial* 2022; 5(10): 13998–14020. <https://doi.org/10.1021/acsanm.2c03477>
32. Khalaji AD: Nano-sized Mercury (II) Schiff Base Complexes: Synthesis, Characterization and Thermal Studies. *Chemical Methodologies* 2020; 4: 34-39. <https://doi.org/10.33945/SAMI/CHEMM.2020.1.3>
33. Pallai DB, Bedekar RR, Bondge AS, Nagargoge GR, Panchgalle SP and More VS: Synthesis, Spectral and Biological Studies of Co(II), Fe(II), Ni(II), Cu(II), Pd(II), Mn(II), Hg(II), Cd(II), and Zn(II) Complexes Derived from Benzohydrazide Schiff Base. *Journal of Applied Organometallic Chemistry* 2024; 4(1): 76-87. <https://doi.org/10.48309/jaoc.2024.434283.1156>
34. Vijayalakshmi M: Synthesis and spectral characterization of schiff base transition metal complexes, DNA cleavage and antibacterial activity studies. *Rasayan Journal of Chemistry* 2018; 11(2): 857-864. <https://doi.org/10.31788/RJC.2018.1123033>.
35. Ravula MR: Synthesis, characterization and antimicrobial activity of Schiff base ligand and Metal complexes. *Indian Journal of Chemistry* 2024; 63(3): 281-285. <https://doi.org/10.56042/ijc.v63i3.6539>
36. George AA and Lokhande MV: Spectral Studies of New Organometallic Schiff Base Complexes and their Anti-Fungal Activity. *International Journal of Pharmaceutical Science and Research* 2017; 8(8): 3413-3420. [https://doi.org/10.13040/IJPSR.0975-8232.8\(8\).3413-20](https://doi.org/10.13040/IJPSR.0975-8232.8(8).3413-20)
37. Drosou M, Mitsopoulou CA, Orio M and Pantazis DA, EPR Spectroscopy of Cu(II) Complexes: Prediction of g-Tensors Using Double-Hybrid Density Functional Theory. *Magnetochemistry* 2022; 8: 36. <https://doi.org/10.3390/magnetochemistry8040036>
38. Hashem H, Mohamed E, Farag AA and Azmy E: New heterocyclic Schiff base-metal complex: Synthesis, characterization, density functional theory study, and antimicrobial evaluation. *Applied Organometallic Chemistry* 2021; 35(9): e6322. <https://doi.org/10.1002/aoc.6322>.
39. Drosou M, Mitsopoulou CA, Orio M and Pantazis DA: EPR Spectroscopy of Cu(II) Complexes: Prediction of g-Tensors Using Double-Hybrid Density Functional Theory. *Magnetochemistry* 2022; 8(36): 1-15. <https://doi.org/10.3390/magnetochemistry8040036>.
40. Chandra S and Gupta M: Spectroscopic characterization and synthesis of Cu(ii) and Ni(ii) complexes with nitrogen and sulphur donor bidentate Schiff's base ligand. *Inter International Journal of Pharmaceutical Science and Research* 2021; 8(2): 8232-8238. [https://doi.org/10.13040/IJPSR.0975-8232.8\(2\).679-85](https://doi.org/10.13040/IJPSR.0975-8232.8(2).679-85).

How to cite this article:

Kapade MG, Batawale PP, Dalvi UM and Lokhande MV: Synthesis and characterization of noval schiff base complexes of MN(II), CO(II), NI(II), CU(II), ZN(II), PD(II), PT(II) metal ions for microbial activities and their nanoparticles. *Int J Pharm Sci & Res* 2024; 15(11): 3297-06. doi: 10.13040/IJPSR.0975-8232.15(11).3297-06.

All © 2024 are reserved by International Journal of Pharmaceutical Sciences and Research. This Journal licensed under a Creative Commons Attribution-NonCommercial-ShareAlike 3.0 Unported License.

This article can be downloaded to **Android OS** based mobile. Scan QR Code using Code/Bar Scanner from your mobile. (Scanners are available on Google Playstore)